

FAST OPED ALGORITHM FOR RECONSTRUCTION OF IMAGES FROM RADON DATA

YUAN XU AND OLEG TISCHENKO

ABSTRACT. A fast implementation of the OPED algorithm, a reconstruction algorithm for Radon data introduced recently, is proposed and tested. The new implementation uses FFT for discrete sine transform and an interpolation step. The convergence of the fast implementation is proved under the condition that the function is mildly smooth. The numerical test shows that the accuracy of the OPED algorithm changes little when the fast implementation is used.

1. INTRODUCTION

Reconstruction images from Radon data is the central theme in medical imaging. The dominating reconstruction method, or algorithm, currently used for this task is FBP (filtered backprojection) method. A new reconstruction algorithm, called OPED, was introduced recently as a possible alternative in [12] and studied further in [9, 13]. OPED is based on orthogonal polynomial expansions on the disk, which is fundamentally different from FBP. Our study has indicated a number of potential advantages of OPED vs FBP. The purpose of this paper is to show that OPED can compete with FBP in speed as well.

Fast reconstruction is one of the reasons that FBP is widely used. The structure of the FBP algorithm contains a discrete convolution, which can be evaluated with FFT (fast Fourier transform). Together with an interpolation step, this ensures that FBP algorithm can be implemented efficiently. In contrast, the OPED algorithm does not use discrete convolutions. Nevertheless, it uses Chebyshev polynomials of the second kind, which turns out to allow an implementation with similar combination of FFT and interpolation, except that we will use fast discrete sine transforms instead. The result is a fast implementation of OPED algorithm, comparable to the implementation of FBP in the number of operations.

The additional interpolation step will introduce an error in the reconstruction. It turns out, however, that the additional error is small. The convergence of the OPED algorithm is proved theoretically under mild condition on the function that represents the image. Treating the approximation provided by the algorithm as an operator, denoted by \mathcal{A}_{2m} , from the space of continuous functions to itself, the proof in [12] amounts to show that the operator norm of \mathcal{A}_{2m} is exactly $\|\mathcal{A}_{2m}\| = \mathcal{O}(m \log(m+1))$, where $2m+1$ is the number of views of the Radon projections. It turns out, as we shall show, that the order of the norm remains to be the same even

Date: July 27, 2021.

1991 Mathematics Subject Classification. 42C15, 65D15.

Key words and phrases. OPED algorithms, reconstruction of images, Radon data, polynomials of two variables.

The first author was partially supported by the National Science Foundation under Grant DMS-0604056.

when the interpolation step is used. The OPED algorithm preserves polynomials of degree $2m - 1$, so that the order of $\|\mathcal{A}_{2m}\|$ implies that the algorithm converges uniformly if the function is mildly smooth, say, if the function has continuous second order derivatives. The OPED with interpolation step no longer preserves polynomials. Nevertheless, we shall show that the convergence still holds for smooth functions, say for functions that have fourth continuous derivatives. We also test the fast implementation of OPED numerically. The result shows that the speed of fast implementation is improved in the order of magnitude, while the quality of the reconstruction changes little even for images that have sharp jumps.

The paper is organized as follows. We describe OPED algorithm and its fast implementation in the following section. The convergence of the fast OPED algorithm is established in Section 3. The numerical testing and examples are given in Section 4.

2. OPED ALGORITHM AND ITS FAST IMPLEMENTATION

2.1. OPED algorithm. A two dimensional image on the unit disk $B = \{(x, y) : x^2 + y^2 \leq 1\}$ is represented by a function $f(x, y)$ defined on B . A Radon projection of f is a line integral,

$$\mathcal{R}f(\theta, t) := \int_{I(\theta, t)} f(x, y) dx dy, \quad 0 \leq \theta \leq 2\pi, \quad -1 \leq t \leq 1,$$

where $I(\theta, t) = \{(x, y) : x \cos \theta + y \sin \theta = t\} \cap B$ is a line segment inside B . The essential problem of image reconstruction from Radon data is to recover the image represented by $f(x, y)$ from a finite collection of its Radon projections.

OPED is a reconstruction algorithm based on orthogonal expansion on the disk. Let $\mathcal{V}_n(B)$ denote the space of orthogonal polynomials of degree n on B with respect to the Lebesgue measure. A function in $L^2(B)$ can be expanded in terms of orthogonal polynomials, that is,

$$(2.1) \quad f(x) = \sum_{k=0}^{\infty} \text{proj}_k f(x), \quad \text{proj}_k : L^2(B) \mapsto \mathcal{V}_n(B).$$

The partial sum of this expansion is $S_n f(x) = \sum_{k=0}^n \text{proj}_k f(x, y)$, which provides a natural approximation to f . It is shown in [12] that the partial sum can be expressed directly in terms of Radon projections:

$$(2.2) \quad S_{2m} f(x, y) = \frac{1}{2m+1} \sum_{\nu=0}^{2m} \frac{1}{\pi} \int_{-1}^1 \mathcal{R}f(\phi_\nu, t) \Phi_\nu(t; x, y) dt$$

where $\phi_\nu = \frac{2\pi\nu}{2m+1}$,

$$\Phi_\nu(t; x, y) = \frac{1}{2m+1} \sum_{k=0}^{2m} (k+1) U_k(t) U_k(x \cos \phi_\nu + y \sin \phi_\nu),$$

and $U_k(t)$ denote the Chebyshev polynomial of the second kind,

$$(2.3) \quad U_k(t) = \frac{\sin(k+1)\theta}{\sin \theta}, \quad t = \cos \theta.$$

It turns out that the formula (2.2) can be found implicitly in [3] (see (5.9), (4.3) and (3.7) there). Furthermore, a double integral expression for $S_n f$ can be found in [1, 7] from which (2.2) can be deduced by a quadrature on the unit circle.

Using a quadrature to discretize the integral over t gives an approximation to f based on discrete Radon data. A particular choice of the quadrature formula gives the OPED algorithm:

OPED Algorithm. *Let m be a positive integer. For each reconstruction point $(x, y) \in B$,*

$$(2.4) \quad \mathcal{A}_{\text{OPED}} := \sum_{\nu=0}^{2m} \sum_{j=0}^{2m} g_{j,\nu} T_{j,\nu}(x, y), \quad g_{j,\nu} =: \mathcal{R}f(\phi_\nu, \cos \psi_j),$$

where $\phi_\nu = \frac{2\nu\pi}{2m+1}$, $\psi_j = \frac{(2j+1)\pi}{4m+2}$, and

$$(2.5) \quad T_{j,\nu}(x, y) = \frac{1}{(2m+1)^2} \sum_{k=0}^{2m} (k+1) \sin(k+1) \psi_j U_k(x \cos \phi_\nu + y \sin \phi_\nu).$$

The above version of OPED will be referred to as OPED of type I as it comes from Gaussian quadrature based on the zeros $\cos \frac{(2j+1)\pi}{4m+2}$, $0 \leq j \leq 2m$, of the Chebyshev polynomial of the first kind. An alternative is the OPED of type II, which uses Gaussian quadrature based on the zeros, $\cos \frac{j\pi}{2m+1}$, $1 \leq j \leq 2m$, of the Chebyshev polynomials of the second kind, for which the sum over j in (2.4) should start from $j = 1$ and ψ_j should be replaced by $\psi_j = \frac{j\pi}{2m+1}$. These two choices lead to different scanning geometry of x-ray data, the advantage of the first type is explained in [9]. Unless specifically stated, OPED in the following means type I. The type II case will be mentioned whenever appropriate, the proof can be worked out in the same way and will be omitted.

For each (x, y) in the domain B , the algorithm produces a number $\mathcal{A}_{\text{OPED}}$ which approximates the value of the image at that point. Typically a larger m produces a better approximation. The values of $\mathcal{A}_{\text{OPED}}$ on the reconstruction points, say on a grid of pixel points, give the reconstruction of the image. The convergence of the OPED algorithm is equivalent to the approximation property of the linear operator

$$(2.6) \quad \mathcal{A}_{2m}f(x, y) = \sum_{\nu=0}^{2m} \sum_{j=0}^{2m} \mathcal{R}f(\phi_\nu, \cos \psi_j) T_{j,\nu}(x, y)$$

where f is the function that represents the image. The operator \mathcal{A}_{2m} preserves polynomials of degree $2m - 1$, that is, $\mathcal{A}_{2m}f \equiv f$ if f is a polynomial of degree at most $2m - 1$. In other words, the algorithm produces an image exactly if the image happens to be represented by a polynomial of degree less than $2m - 1$. Furthermore, let $\|\mathcal{A}_{2m}\|$ denote the operator norm of \mathcal{A}_{2m} in the uniform norm over B ; then ([12])

$$(2.7) \quad \|\mathcal{A}_{2m}\| = \mathcal{O}(m \log(m+1)), \quad \text{as } m \rightarrow \infty.$$

As a consequence of this estimate, it follows that $\mathcal{A}_{2m}f$ converges uniformly to f on the disk B if f has continuous second order derivatives. The numerical test has shown that OPED gives fairly accurate reconstruction even when the data has sharp singularities. The proof of (2.7) is based on the following compact formula of $T_{j,\nu}(x, y)$.

Proposition 2.1. *Let $\theta_\nu := \theta_\nu(x, y)$. Then*

$$(2m+1)^2 T_{j,\nu}(x, y) = \frac{(-1)^j (2m+1) \sin(2m+1)\theta_\nu}{2 \sin \theta_\nu} - \frac{(-1)^j (2m+1) \cos(2m+1)\theta_\nu}{\cos \psi_j - \cos \theta_\nu} - \frac{\sin \theta_\nu \sin \psi_j - (-1)^j \sin(2m+1)\theta_\nu (1 - \cos \theta_\nu \cos \psi_j)}{2 \sin \theta_\nu (\cos \psi_j - \cos \theta_\nu)^2}.$$

It should be mentioned that (2.7) was proved in [12] for OPED of type II. The compact formula of $T_{j,\nu}$ in [12] is also established for type II. So, the formula of $T_{j,\nu}$ in the above proposition and (2.7) are in fact new, but the proof is very much similar to that of [12] and we choose not to repeat it.

The use of orthogonal expansion in reconstructing functions from their Radon data can be traced back to the classical paper of Cormack, whose Radon inversion formula is based on the expansions of f and Rf in spherical harmonics ([6, p. 25]). The orthogonal polynomials on the disk have been used in the papers [3, 5] and in the singular value decomposition of Radon transforms (see [6]). The formula (2.2) and the resulted OPED algorithm are introduced in [12]. As we mentioned before that (2.2) itself can be deduced from [3] as well as BG,P. The OPED of type II is closely related to an algorithm in [2]. The connection to orthogonal polynomial expansion was not considered in [2], nor was the convergence studied there. For other algorithms and image reconstruction based on polynomial approximation, see [3, 4, 5, 6] and the references therein.

2.2. Fast implementation of OPED algorithm. The structure of the \mathcal{A}_{2m} in (2.4) allows us to use FFT (fast Fourier transform) once in a straightforward manner. In fact, let us define

$$S_{k,\nu} = \frac{k+1}{(2m+1)^2} \sum_{j=0}^{2m} g_{j,\nu} \sin(k+1)\psi_j.$$

Then $S_{k,\nu}$ can be evaluated by FFT for discrete sine transform. We can write $\mathcal{A}_{\text{OPED}}$ as

$$(2.8) \quad \mathcal{A}_{\text{OPED}} = \sum_{\nu=0}^{2m} \sum_{k=0}^{2m} S_{k,\nu} U_k(x \cos \phi_\nu + y \sin \phi_\nu).$$

Thus, the main step of the OPED algorithm lies in the evaluation of the above double sum, which can be considered as a back projection step. Let $N = 2m + 1$. Then the evaluation of the matrix $S_{k,\nu}$ costs $\mathcal{O}(N^2 \log N)$ operations (flops). The evaluation of the double sum costs $\mathcal{O}(N^2)$ operations. Hence, the cost of evaluation on a grid of $M \times M$ is $\mathcal{O}(N^2(M^2 + \log N))$. In particular, if $M \approx N$, then the cost is $\mathcal{O}(N^4)$. The main operation cost is at the evaluation of the double sums at the grid points. In other words, the main cost lies in the back projection step.

Unlike the FBP algorithm, the sum in (2.8) does not contain a discrete convolution that can be evaluated via FFT. However, the formula of U_k in (2.3) allows us to write

$$(2.9) \quad \mathcal{A}_{\text{OPED}}(x, y) = \sum_{\nu=0}^{2m} \frac{1}{\sin \theta_\nu} \sum_{k=0}^{2m} S_{k,\nu} \sin(k+1)\theta_\nu,$$

where

$$\theta_\nu := \theta_\nu(x, y) = \arccos(x \cos \phi_\nu + y \sin \phi_\nu).$$

The inner sum can be evaluated by FFT for discrete sine transform at certain points, which suggests that we introduce an interpolation step to take advantage of the fast evaluation by FFT. To be more precise, we define

$$\alpha_\nu(\theta) = \sum_{k=0}^{2m} S_{k,\nu} \sin(k+1)\theta, \quad 0 \leq \theta \leq \pi,$$

after the inner sum of (2.9). The FFT for discrete sine transforms can be used to evaluate the numbers

$$\alpha_{l,\nu} := \alpha_\nu(\xi_l), \quad \xi_l := \frac{(l+1)\pi}{2m+1}, \quad l = 0, 1, \dots, 2m-1$$

effectively. That is, the inner sum in (2.9) can be evaluated by FFT when $\theta_\nu(x, y) = \xi_l$. For the interpolation step, we choose linear interpolation, which is also used in the implementation of FBP [6, p. 109]. For a given (x, y) , we choose the integer l such that $\theta_\nu(x, y)$ lies between ξ_l and ξ_{l+1} and use the value of the linear interpolation between $\alpha_{l,\nu}$ and $\alpha_{l+1,\nu}$ as an approximation to the inner sum of (2.9). The linear interpolation is given by

$$(2.10) \quad \ell_\nu(\theta) = u_\nu(\theta)\alpha_{l+1,\nu} + (1 - u_\nu(\theta))\alpha_{l,\nu}, \quad u_\nu(\theta) := \frac{\theta - \xi_l}{\xi_{l+1} - \xi_l},$$

where $\xi_l \leq \theta \leq \xi_{l+1}$. Then the fast implementation of OPED is given as follows:

Fast OPED algorithm: Let m be a positive integer.

Step 1. For each $\nu = 0, \dots, 2m$, use FFT to compute for each $k = 0, \dots, 2m$,

$$S_{k,\nu} = \frac{k+1}{(2m+1)^2} \sum_{j=0}^{2m} g_{j,\nu} \sin(k+1)\psi_j.$$

Step 2. For each $l = 0, 1, \dots, 2m-1$, use FFT to compute

$$\alpha_{l,\nu} := \sum_{k=0}^{2m} S_{k,\nu} \sin(k+1)\xi_l.$$

Step 3. For each reconstruction point (x, y) inside the disk of the radius $\cos \frac{\pi}{2m+1}$, determine integers l such that

$$l = \left\lfloor \frac{2m+1}{\pi} \theta_\nu \right\rfloor - 1, \quad \text{where } \theta_\nu = \arccos(x \cos \phi_\nu + \sin \phi_\nu),$$

and evaluate

$$f_{\text{OPED}} = \sum_{\nu=0}^{2m} \frac{1}{\sin \theta_\nu} [(1 - u_\nu)\alpha_{l,\nu} + u_\nu\alpha_{l+1,\nu}],$$

where $u_\nu = (2m+1)\theta_\nu/\pi - (l+1)$.

A fast implementation for OPED of type II works similarly, with ξ_l replaced by $\xi = \frac{(l+\frac{1}{2})\pi}{2m+1}$, $0 \leq l \leq 2m$. In other words, exchanging the values of ψ_j and ξ_l in the above fast algorithm for OPED of type I leads to the fast algorithm for OPED of type II.

A couple of remarks are in order. First of all, $\sin \theta_\nu$ appears in the denominator in the last step of the algorithm. However, $\sin \theta_\nu = 0$ only if $\cos \theta_\nu(x, y) = x \cos \phi_\nu + y \sin \phi_\nu = 1$, which happens only if $(x, y) = (\cos \phi_\nu, \sin \phi_\nu)$. Since the points $(\cos \phi_\nu, \sin \phi_\nu)$ are on the boundary of the region B , we do not have to take them

as reconstruction points. In fact, the region of interests is usually inside the unit disk; thus, we can evaluate at points inside a smaller disk in B , and this will also ensure that the values of $\sin \theta_\nu$ in the last step will not be too small to cause loss of significant digits in the computation. Furthermore, if we restrict (x, y) to a disk with radius $\cos \xi_0 = \cos \pi/(2m+1)$, then it will also guarantee that the choice of l in the Step 3 is unique for all (x, y) in that disk.

The algorithm uses FFT twice, the final sum in Step 3 is a single sum whose evaluation costs $\mathcal{O}(N)$ operations. Hence, the cost of evaluations on an $M \times M$ grid with $M \approx N$ is $\mathcal{O}(N^3)$, which is in the same order of magnitude as the FBP algorithm. In fact, the structure of the OPED algorithm with this fast implementation is similar to that of FBP algorithm (cf. [6, p. 109]).

3. CONVERGENCE OF OPED ALGORITHM WITH LINEAR INTERPOLATION

Throughout this section, we let $\|\cdot\|$ denote the uniform norm on B .

As we mentioned before that the convergence of the OPED algorithm depends on the norm \mathcal{A}_{2m} of the operator defined in (2.6). Following the proof in [12], we have

$$\|\mathcal{A}_{2m}\| = \max_{(x,y) \in B} \sum_{\nu=0}^{2m} \sum_{j=0}^{2m} \sin \psi_j |T_{j,\nu}(x, y)| = \mathcal{O}(m \log(m+1)).$$

As a consequence of this estimate and the fact that \mathcal{A}_{2m} preserves polynomials of degree $2m-1$, the triangle inequality implies that

$$(3.1) \quad \|\mathcal{A}_{2m}f - f\| \leq cm \log(m+1) E_{2m-1}(f)$$

where $E_n(f) = \inf\{\|f - P_n\| : \deg P_n \leq n\}$ is the error of best approximation to f by polynomials of degree at most n . It is known ([11]) that if $f \in C^{2r}(B)$, then

$$(3.2) \quad E_n(f) \leq cn^{-2r} \|\mathcal{D}^r f\|,$$

where \mathcal{D} is a differential operator of order $2r$. In particular, (3.1) and (3.2) show that $\mathcal{A}_{2m}f$ converges uniformly to f if f has continuous second order derivatives.

When the interpolation step is used in the evaluation of OPED, the operator is changed and we denote the new operator by \mathcal{AI}_{2m} , which is given by

$$\mathcal{AI}_{2m}f(x, y) := \sum_{\nu=0}^{2m} \frac{1}{\sin(\theta_\nu(x, y))} \ell_\nu(\theta_\nu(x, y)),$$

where ℓ_ν is defined in (2.10). It turns out that the norm of the operator \mathcal{AI}_{2m} has the same growth order as that of \mathcal{A}_{2m} .

Proposition 3.1. *For $m \geq 0$, let $\Omega_m = \{(x, y) : \sqrt{x^2 + y^2} \leq \cos \pi/(2m+1)\}$. Then*

$$\max_{(x,y) \in \Omega_m} |\mathcal{AI}_{2m}f(x, y)| \leq c\|f\| m(\log(m+1)).$$

Proof. Let $u_\nu = (\theta_\nu - \xi_l)/(\xi_{l+1} - \xi_l)$. The way that the index l is chosen implies that $0 \leq u_\nu \leq 1$. Recall the definition of $T_{j,\nu}(x, y)$ in (2.5). We shall abuse the notation somewhat and write $T_{j,\nu}(\xi_l)$ when $\arccos(x \cos \phi_\nu + y \sin \phi_\nu) = \xi_l$. Using

the definition of $U_n(t)$ in (2.3), the operator can be written as

$$\begin{aligned} \mathcal{AI}_{2m}f(x, y) &= \sum_{\nu=0}^{2m} \frac{1}{\sin \theta_\nu(x, y)} \sum_{j=0}^{2m} \mathcal{R}f(\phi_\nu, \cos \psi_j) \\ &\quad \times [(1 - u_\nu)T_{j,\nu}(\xi_l) \sin \xi_l + u_\nu T_{j,\nu}(\xi_{l+1}) \sin \xi_{l+1}]. \end{aligned}$$

For $(x, y) \in \Omega_m$, write $x = r \cos \phi$ and $y = r \sin \phi$, then $x \cos \phi_\nu + y \sin \phi_\nu = r \cos(\phi - \phi_\nu) \leq r$ and $r \leq \cos \pi/(2m+1)$. In particular,

$$(3.3) \quad \sin \theta_\nu(x, y) = \sqrt{1 - \cos^2 \theta_\nu(x, y)} \geq \sqrt{1 - \cos^2 \frac{\pi}{2m+1}} = \sin \frac{\pi}{2m+1}.$$

Furthermore, the definition of ξ_l shows that there is a constant c independent of m such that

$$\left| \frac{\sin \xi_l}{\sin(\theta_\nu(x, y))} \right| \leq c \quad \text{and} \quad \left| \frac{\sin \xi_{l+1}}{\sin(\theta_\nu(x, y))} \right| \leq c$$

for $(x, y) \in \Omega_m$. Consequently, we conclude that

$$(3.4) \quad |\mathcal{AI}_{2m}f(x, y)| \leq \sum_{\nu=0}^{2m} \sum_{j=0}^{2m} |\mathcal{R}f(\phi_\nu, \cos \psi_j)| (|T_{j,\nu}(\xi_l)| + |T_{j,\nu}(\xi_{l+1})|).$$

Using the fact that $|\mathcal{R}f(\phi, t)| \leq \sqrt{1 - t^2} \|f\|$ (see, for example, [12]), it follows that

$$|\mathcal{AI}_{2m}f(x, y)| \leq \|f\| \sum_{\nu=0}^{2m} \sum_{j=0}^{2m} \sin \psi_j (|T_{j,\nu}(\xi_l)| + |T_{j,\nu}(\xi_{l+1})|).$$

We now use the compact formula of $T_{j,\nu}$ in Proposition 2.1. Since $\sin(2m+1)\xi_l = 0$ and $\cos(2m+1)\xi_l = (-1)^{l+1}$, it follows that

$$(2m+1)^2 T_{j,\nu}(\xi_l) = -\frac{(-1)^{j+l+1}(2m+1)}{\cos \psi_j - \cos \xi_l} - \frac{(-1)^{l+1} \sin \psi_j}{2(\cos \psi_j - \cos \xi_l)^2}.$$

Since $\phi_j = \frac{(j+1/2)\pi}{2m+1}$ and $\xi_l = \frac{(l+1)\pi}{2m+1}$, the denominator of $T_{j,\nu}(\xi_l)$ is never zero. We have

$$\cos \psi_j - \cos \xi_l = 2 \sin \frac{\xi_l - \psi_j}{2} \sin \frac{\xi_l + \psi_j}{2}.$$

Since $\psi_{2m-j} = \pi - \psi_j$ and $\xi_{2m-l} = \pi - \xi_{l-1}$, we can assume that $0 < \xi_l < \pi/2$, which means that $0 \leq l \leq m-1$. If $0 \leq \psi_j \leq \pi/2$, we have

$$\frac{\sin \psi_j}{\sin \frac{\psi_j + \xi_l}{2}} = 2 \frac{\sin \frac{\psi_j}{2} \cos \frac{\psi_j}{2}}{\sin \frac{\psi_j + \xi_l}{2}} \leq 2 \cos \frac{\psi_j}{2} \leq 2.$$

The above equation also holds if $\pi/2 < \psi_j < \pi$, since then $\pi/4 \leq \frac{\psi_j + \xi_l}{2} \leq 3\pi/4$ and $\sin \frac{\psi_j + \xi_l}{2} \geq \sqrt{2}/2$. Hence, using the fact that $\sin \theta \geq (2/\pi)\theta$ for $0 \leq \theta \leq \pi/2$

we have

$$\begin{aligned}
\sum_{\nu=0}^{2m} \sum_{j=0}^{2m} \sin \psi_j |T_{j,\nu}(\xi_l)| &\leq \sum_{j=0}^{2m} \frac{1}{|\sin \frac{\psi_j - \xi_l}{2}|} + \frac{1}{2m+1} \sum_{j=0}^{2m} \frac{1}{|\sin \frac{\psi_j - \xi_l}{2}|^2} \\
&\leq \pi \sum_{j=0}^{2m} \frac{1}{|\psi_j - \xi_l|} + \frac{\pi^2}{2m+1} \sum_{j=0}^{2m} \frac{1}{|\psi_j - \xi_l|^2} \\
&\leq \sum_{j=0}^{2m} \frac{2m+1}{|j-l+1/2|} + \sum_{j=0}^{2m} \frac{2m+1}{|j-l+1/2|^2} \\
&\leq c(2m+1) \log(m+1).
\end{aligned}$$

The sum involving $T_{j,\nu}(\xi_{l+1})$ is estimated in exactly the same way. By (3.4), the proof is completed. \square

This proposition shows that the interpolation step does not increase the growth order of the operator norm, at least when we restrict the norm to the region Ω_m . Unlike \mathcal{A}_{2m} , the operator \mathcal{AI}_{2m} no longer preserves polynomials of high degrees. We need an estimate of the error $\mathcal{AI}_{2m}f - f$ for f being a polynomial. First, however, we need some results on $\text{proj}_k : L^2(B) \mapsto \mathcal{V}_k(B)$ defined in (2.1). Let $P_n(\mathbf{x}, \mathbf{y})$, $\mathbf{x}, \mathbf{y} \in B$, denote the reproducing kernel of $\mathcal{V}_k(B)$. Then

$$\text{proj}_k f(\mathbf{x}) = \frac{1}{\pi} \int_B f(\mathbf{y}) P_k(\mathbf{x}, \mathbf{y}) d\mathbf{y}.$$

Furthermore, the kernel P_k satisfies a compact formula ([10])

$$(3.5) \quad P_k(\mathbf{x}, \mathbf{y}) = \frac{k+1}{2} \int_0^\pi U_k(\langle \mathbf{x}, \mathbf{y} \rangle + s\sqrt{1-\|\mathbf{x}\|^2}\sqrt{1-\|\mathbf{y}\|^2}) \frac{ds}{\sqrt{1-s^2}},$$

where $\langle \cdot, \cdot \rangle$ and $\|\cdot\|$ are the usual Euclidean inner product and norm on \mathbb{R}^2 , and U_k is the Chebyshev polynomial of the second kind.

Lemma 3.2. *Let $\|f\|_2$ denote the $L^2(B)$ norm of f . Then the projection operator satisfies*

$$|\text{proj}_k f(\mathbf{x})| \leq (k+1)\|f\|_2, \quad \forall \mathbf{x} \in B.$$

Proof. Using the Cauchy-Schwartz inequality and the reproducing property of $P_k(\cdot, \cdot)$, we have

$$|\text{proj}_k f(\mathbf{x})| \leq \|f\|_2 \left(\frac{1}{\pi} \int_B |P_k(\mathbf{x}, \mathbf{y})|^2 d\mathbf{y} \right)^{1/2} = \|f\|_2 [P_k(\mathbf{x}, \mathbf{x})]^{1/2}.$$

The definition (2.3) gives the well known inequality $|U_k(t)| \leq k+1$, so that by (3.5) we have $|P_k(\mathbf{x}, \mathbf{x})| \leq (k+1)^2$, from which the stated result follows. \square

Using $\text{proj}_k f$ we can construct a sequence of polynomials that approximates f . For this we let η be a nonnegative C^∞ function on \mathbb{R} that satisfies

$$\eta(t) = 1, \quad 0 \leq t \leq 1, \quad \text{and} \quad \text{supp } \eta(t) = [0, 2].$$

For $f \in L^2(B)$ we define $S_n^\eta f$ by

$$S_n^\eta f(\mathbf{x}) = \sum_{j=0}^{2n} \eta\left(\frac{j}{n}\right) \text{proj}_j f(\mathbf{x}).$$

Let Π_n^2 denote the space of polynomials of degree at most n in two variables. The approximation property of S_n^η is given in the following lemma ([11]).

Lemma 3.3. *Let $f \in C(B)$. Then*

- (1) $S_n^\eta f \in \Pi_{2n-1}^2$ and $S_n^\eta P = P$ for $P \in \Pi_n^2$;
- (2) for $n \in \mathbb{N}$,

$$\|S_n^\eta f\| \leq c\|f\| \quad \text{and} \quad \|f - S_n^\eta f\| \leq cE_n(f).$$

This shows that $S_n^\eta f$ realizes, up to a constant, the best approximation by polynomials. For this sequence of polynomials, we have the following:

Lemma 3.4. *Let $F = S_q^\eta$ and $q < m$. For each compact subset Ω in B , there is a constant c , independent of q , m and f , such that*

$$\max_{(x,y) \in \Omega} |\mathcal{A}_{2m} F(x,y) - F(x,y)| \leq c\|f\| \frac{q^4}{(2m+1)^2}.$$

Proof. Since F is a polynomial of degree $2q$, we write its expansion as

$$F(x,y) = \sum_{j=0}^{2q} F_j(x,y), \quad F_j = \eta \binom{j}{q} \text{proj}_j f(x) \in \mathcal{V}_j(B).$$

The Radon projections of orthogonal polynomials can be explicitly computed. We have ([5]),

$$\mathcal{R}F_j(\phi, t) = \frac{2}{j+1} \sqrt{1-t^2} U_j(t) F_j(\cos \phi, \sin \phi).$$

The polynomials $U_k(t)$ are orthogonal with respect to $\sqrt{1-t^2}$ on the interval $[-1, 1]$. Consequently,

$$\frac{1}{\pi} \int_{-1}^1 \mathcal{R}F_j(\phi, t) U_k(t) dt = \frac{1}{k+1} F_j(\cos \phi, \sin \phi) \delta_{k,j}.$$

Hence, using (2.2) and the fact that $q < m$, we conclude that

$$\begin{aligned} (3.6) \quad F(x,y) &= S_{2m} F(x,y) = \sum_{j=0}^{2q} S_{2m} F_j(x,y) \\ &= \frac{1}{2m+1} \sum_{\nu=0}^{2m} \sum_{j=0}^{2q} F_j(\cos \phi_\nu, \sin \phi_\nu) U_j(\cos \theta_\nu(x,y)). \end{aligned}$$

In exactly the same way, we also obtain that

$$\begin{aligned} (3.7) \quad \mathcal{A}_{2m} f(x,y) &= \frac{1}{2m+1} \sum_{\nu=0}^{2m} \frac{1}{\sin \theta_\nu(x,y)} \sum_{j=0}^{2q} F_j(\cos \phi_\nu, \sin \phi_\nu) \\ &\quad \times [(1-u_\nu) \sin(j+1)\xi_{l+1} + u_\nu \sin(j+1)\xi_l], \end{aligned}$$

where $u_\nu = u_\nu(\theta_\nu(x,y))$ is the linear function in (2.10). Introducing the function

$$H_\nu(\theta) = \sum_{j=0}^{2q} F_j(\cos \phi_\nu, \sin \phi_\nu) \sin(j+1)\theta,$$

which depends on F , we then conclude that

$$\begin{aligned} & F(x, y) - \mathcal{AI}_{2m}F(x, y) \\ &= \frac{1}{2m+1} \sum_{\nu=0}^{2m} \frac{1}{\sin \theta_\nu(x, y)} [H_\nu(\theta_\nu(x, y)) - (1 - u_\nu)H_\nu(\xi_l) - u_\nu H_\nu(\xi_{l+1})]. \end{aligned}$$

The expression in the square bracket is the difference of $H_\nu(\cdot)$ and its linear interpolation at ξ_l and ξ_{l+1} evaluated at $\theta_\nu(x, y)$. Hence the well-known estimate of the error of linear interpolation shows

$$\begin{aligned} & |H_\nu(\theta_\nu(x, y)) - (1 - u_\nu)H_\nu(\xi_l) - u_\nu H_\nu(\xi_{l+1})| \\ & \leq \frac{1}{2} \|H_\nu''\| |(\theta_\nu(x, y) - \xi_l)(\theta_\nu(x, y) - \xi_{l+1})| \leq \frac{1}{16} \|H_\nu''\| \frac{\pi^2}{(2m+1)^2}, \end{aligned}$$

where $\|H_\nu''\| = \max_{0 \leq \theta \leq \pi} |H_\nu''(\theta)|$. Since H_ν is a trigonometric polynomial of degree $2q$, the classical Bernstein inequality (cf. [14, Vol. 2, p. 11]) shows that

$$\|H_\nu''\| \leq (2q)^2 \|H_\nu\| := 2q^2 \max_{0 \leq t \leq \pi} |H_\nu(t)|.$$

Furthermore, by the definition of H_ν and Lemma 3.2, we have

$$\begin{aligned} \|H_\nu\| & \leq \sum_{j=0}^{2q} |F_j(x, y)| \leq \sum_{j=0}^{2q} |\text{proj}_j F(x, y)| \\ & \leq \|f\|_2 \sum_{j=0}^{2q} (j+1) \leq 2(q+1)^2 \|f\|. \end{aligned}$$

Hence, putting these inequalities together, we conclude that

$$|F(x, y) - \mathcal{AI}_{2m}F(x, y)| \leq c \|f\| \frac{q^4}{(2m+1)^3} \sum_{\nu=0}^{2m} \frac{1}{\sin \theta_\nu(x, y)}.$$

If $(x, y) \in \Omega$, a compact set in B , then there is an $r < 1$ such that $\sqrt{x^2 + y^2} \leq r$, so that $\sin \theta_\nu(x, y) \geq \sqrt{1 - r^2}$ as in (3.3). Thus the last sum is bounded by a constant multiple of m and the stated result follows. \square

Theorem 3.5. *If $f \in C^4(B)$ and Ω is a compact subset of B , then there is a constant c_f , independent of m , such that*

$$(3.8) \quad \max_{(x, y) \in \Omega} |\mathcal{AI}_{2m}f(x, y) - f(x, y)| \leq c_f \frac{\log(m+1)}{\sqrt{m}}.$$

In particular, $\mathcal{AI}_{2m}f$ converges uniformly to f on any compact subset of B .

Proof. Let $F = S_q^\eta f$ and $q < m$ as in the previous lemma and Ω be a compact subset of B . Since \mathcal{AI}_{2m} is a linear operator, by the triangle inequality, Proposition 3.1, Lemma 3.3 and Lemma 3.4, we obtain

$$\begin{aligned} |\mathcal{AI}_{2m}f(x, y) - f(x, y)| & \leq (1 + \|\mathcal{AI}_{2m}\|) |(f - F)(x, y)| + |\mathcal{AI}_{2m}F(x, y) - F(x, y)| \\ & \leq c (m \log(m+1) E_q(f) + m^{-2} q^4 \|f\|) \end{aligned}$$

for all $(x, y) \in \Omega$ and $q < m$. In particular, if $f \in C^4(B)$, then (3.2) implies that

$$(3.9) \quad \max_{(x, y) \in \Omega} |\mathcal{AI}_{2m}f(x, y) - f(x, y)| \leq c (m \log(m+1) q^{-4} \|\mathcal{D}^2 f\| + m^{-2} q^4 \|f\|).$$

In particular, setting $q \approx m^{3/8}$ in the above inequality gives (3.8). \square

The theorem is stated for functions in $C^4(B)$, which is likely too restrictive and the convergence could hold under less restrictive conditions. Also, for functions that are more smooth, one could get better convergence rate by choosing q in (3.9) differently. The rate so obtained and the one in (3.8), however, are likely not sharp and reflect the limitation of our method of proof.

The main merit of the theorem is that it establishes the convergence of OPED algorithm with linear interpolation for smooth functions (images). In practice, the images often have sharp edges, which means that the functions representing images may not be smooth or even continuous. In the following section we present numerical examples, which demonstrate that $\mathcal{AI}_{2m}f$, OPED with interpolation step, converges well even for functions that are not continuous and it converges almost as well as $\mathcal{A}_{2m}f$, OPED without interpolation step.

4. IMPLEMENTATION AND RESULT

For numerical implementation, we used the FFT for discrete sine transform in the package FFTW (<http://www.fftw.org/>). The numerical example is conducted on the Shepp-Logan head phantom [8] (see Figure 2). This is an analytic phantom, highly singular, as the image contains jumps at the boundary of every ellipse in the image, include the one on the boundary. The function that represents the image is a step function, which is not continuous at the boundary of each of the ellipses.

We reconstruct the image with OPED algorithm without the interpolation step and Fast OPED algorithm, which contains the interpolation step as shown in previous section, respectively. In both cases, $S_{k,\nu}$ are computed with FFT.

In Figure 1 images reconstructed by the original OPED and Fast OPED algorithms are depicted side by side. In these images we choose $m = 512$ and the size of the images are 512×512 pixels.

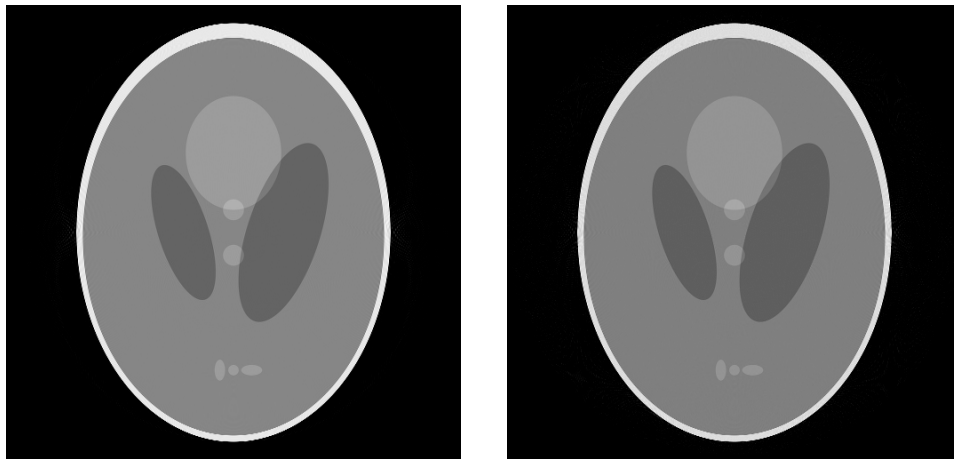


Figure 1. Left: reconstruction by OPED algorithm with $m = 512$. Right: reconstruction by Fast OPED algorithm with $m = 512$.

The reconstruction is carried out on a CELSIUS R610 computer with two Intel Xeon(TM) CPU, each 3065 MHz, and 4 GB RAM. The code is written in C language. Using OPED algorithm, the reconstruction took 344 seconds, in which more than 95% of the time is used on the back projection step. Using Fast OPED algorithm, the reconstruction took merely 13 seconds, an improvement of more that

26 times. Furthermore, the two images show almost no visual difference. In Figure 2, the original Shepp-Logan phantom and the difference of the two images in Figure 1 are depicted.

Figure 2. Left: original Shepp-Logan phantom. Right: the difference between the two reconstructed images in Figure 1.

We can also measure the errors of the reconstruction. Let X denote an image, represented by its pixel values, so that $X = \{X_i : 1 \leq i \leq N\}$, where N is the number of pixels in the image. Let X^R denote the reconstructed image, $X^R = \{X_i^R : 1 \leq i \leq N\}$. The relative square total error (RSE) between X and X^R is defined by

$$Q_{RSE} = \frac{\sum_i (X_i^R - X_i)^2}{\sum_i (X_i^R)^2},$$

and the mean error (ME) between X and X^R is defined by

$$Q_{ME} = \frac{1}{N} \sum_{i=1}^N |X_i - X_i^R|.$$

In our case $N = 512 \times 512 = 512^2$. The result is reported in Table 1, in which ORIG stands for the original Shepp-Logan phantom, OPED and Fast OPED stand for reconstructed image by OPED and by Fast OPED, respectively. For example, ORIG vs OPED means the error between the original phantom and the reconstruction by OPED.

	ORIG vs OPED	ORIG vs FAST OPED	OPED vs FAST OPED
RSE	0.00239702	0.00249574	0.000515499
ME	0.0129175	0.00981329	0.007715128

TABLE 1. Error Estimates of OPED and Fast OPED

The results in the table shows that fast OPED is slightly worse in relative least square error, but slightly better in mean error. The order of magnitude of the error is the same. The difference is practically negligible.

5. CONCLUSION

We introduced a fast implementation of OPED algorithm by using FFT and a linear interpolation step. The fast algorithm is proved to converge uniformly on any compact subset in the disk and the numerical test has shown that it reconstructs images accurately and is as good as the original OPED algorithm.

In conclusion, the fast OPED algorithm with interpolation step is not only much faster, it also shares main merits of the original OPED algorithm. Hence, for practical applications, the fast OPED algorithm should be the recommended method.

REFERENCES

- [1] B. Bojanov and I. K. Georgieva, Interpolation by bivariate polynomials based on Radon projections, *Studia Math.*, **162** (2004), 141 - 160.
- [2] T. Bortfeld and U. Oelfke, Fast and exact 2D image reconstruction by means of Chebyshev decomposition and backprojection, *Phys. Med. Biol.*, **44** (1999), 1105-1120.
- [3] B. Logan, L. Shepp, Optimal reconstruction of a function from its projections, *Duke Math. J.*, **42** (1975), 645-659.
- [4] W. R. Madych, Summability and approximate reconstruction from Radon transform data, *Contemporary Mathematics*, Vol. **113** (1990), 189-219.
- [5] R. Marr, On the reconstruction of a function on a circular domain from a sampling of its line integrals, *J. Math. Anal. Appl.*, **45** (1974), 357-374.
- [6] F. Natterer, *The mathematics of computerized tomography*, Reprint of the 1986 original. Classics in Applied Mathematics, 32. SIAM, Philadelphia, PA, 2001.
- [7] P. Petrushev, Approximation by ridge functions and neural networks, *SIAM J. Math. Anal.* **30** (1999), 155-189.
- [8] L. Shepp and B. Logan, The Fourier reconstruction of a head section, *IEEE Trans. Nucl. Sci.*, **NS-21**, 1974, 21-43.
- [9] O. Tischenko, Yuan Xu and C. Hoeschen, New tomographic reconstruction algorithms, submitted, 2006.
- [10] Yuan Xu, Summability of Fourier orthogonal series for Jacobi weight on a ball in \mathbb{R}^d , *Trans. Amer. Math. Soc.* **351** (1999), 2439-2458.
- [11] Yuan Xu, Weighted approximation of functions on the unit sphere, *Constructive Approx.* **21** (2005), 1-28.
- [12] Yuan Xu, A direct approach for reconstruction of images from Radon projections, *Adv. in Applied Math.*, **36** (2006), 388-420.
- [13] Yuan Xu, O. Tischenko and C. Hoeschen, A new reconstruction algorithm for Radon Data, *Proc. SPIE, Medical Imaging 2006: Physics of Medical Imaging*, vol. **6142**, p. 791-798.
- [14] A. Zygmund, *Trigonometric Series*, Cambridge University Press, 1959.

DEPARTMENT OF MATHEMATICS UNIVERSITY OF OREGON EUGENE, OREGON 97403-1222.
E-mail address: yuan@math.uoregon.edu

INSTITUTE OF RADIATION PROTECTION, GSF - NATIONAL RESEARCH CENTER FOR ENVIRONMENT AND HEALTH, D-85764 NEUHERBERG, GERMANY
E-mail address: oleg.tischenko@gsf.de